

1 **Title page information**

2 **Title:** Simultaneous catalytic de-polymerization and hydrodeoxygenation of lignin in water/formic  
3 acid media with Rh/Al<sub>2</sub>O<sub>3</sub>, Ru/Al<sub>2</sub>O<sub>3</sub> and Pd/Al<sub>2</sub>O<sub>3</sub> as bifunctional catalysts

4 **Authors:** Mikel Oregui Bengoechea<sup>a\*</sup> (double family name), Agnethe Hertzberg<sup>a</sup>, **Nemanja Miletić<sup>b</sup>,**  
5 **Pedro Luis Arias<sup>b</sup>** and Tanja Barth<sup>a</sup>

6 [a] Department of Chemistry, University of Bergen, Norway, Allegaten 41, N-5007 Bergen, Norway

7 [b] Department of Chemical and Environmental Engineering, School of Engineering, University of the  
8 Basque Country (EHU/UPV), C/Alameda Urquijo s/n, 48013 Bilbao, Spain

9

10 \*Corresponding author:

11 Mikel Oregui Bengoechea, Department of Chemistry, University of Bergen, Norway, Allegaten 41, N-  
12 5007 Bergen, Norway. Tel.: +4746230671, email: [mikel.oregui@kj.uib.no](mailto:mikel.oregui@kj.uib.no)

13

14

15 **Abstract**

16 The catalytic solvolysis of 3 lignins of different sources in a formic acid/water media using  
17 bifunctional Ru/Al<sub>2</sub>O<sub>3</sub>, Rh/Al<sub>2</sub>O<sub>3</sub>, Pd/Al<sub>2</sub>O<sub>3</sub> catalysts was explored in a batch set-up at different  
18 temperatures and reaction times (340°C-380°C and 2-6 hours respectively). Blank experiments using  
19 only gamma-alumina as catalysts and non-catalyzed experiments were also performed and compared  
20 with the supported catalysts results. All the supported catalysts significantly improved the oil yields  
21 on a lignin basis, with yields up to 91.5 wt% using the Ru catalyst. The main components phenol,  
22 cresol, guaiacol, methylguaiacol, catechol, ethylcatechol, syringol and o-vanillin are found in different  
23 concentrations depending on the catalytic system. The stable Lewis acidity in the alumina support  
24 has been found to be active in terms of de-polymerization of lignin, leading to lower average  
25 molecular weight oils. In addition, it was found that alumina plays a significant role in the re-  
26 polymerization mechanism of the monomers. The effect of the type of lignin on the final oil and solid  
27 yields was also established, demonstrating that **lignins produced by basic pretreatment of biomass**  
28 **do not show significant increase in oil yield when catalysts on an acid support like alumina are used.**  
29 **The interpretation is that acid conditions are needed for efficient de-polymerisation of the lignin.**

30

31 **Keywords**

32 Catalytic hydrotreatment; solvolysis; lignin; noble metals; alumina; bifunctional heterogeneous  
33 catalysis

34

35

36

## 37 1. Introduction

38 In the biofuel sector, the concept of a “biorefinery” describes all the processes and technologies  
39 involved in converting biomass to a range of fuels and value-added chemicals. Among the biomass  
40 sources, lignocellulosic biomass (wood, grasses and agricultural residues) has been identified as a  
41 promising alternative for this purpose [1], since unlike vegetable oil and sugar crops the  
42 lignocellulose feedstock avoid the negative side effect of intense farming [2] and ethical concerns  
43 about the use of food as fuel raw materials [3]. For lignocellulosic biomass conversion, most of the  
44 research has been focused on the conversion of cellulose and hemi-cellulose to biofuels and value  
45 added chemicals, and major breakthroughs have been achieved. However, valorization of lignin, an  
46 amorphous polymer that accounts for 15-30% of the feedstock by weight, and 40 % by energy [1], is  
47 still a challenge. Only approximately 2% of the lignin residues available from the pulp and paper  
48 industry are used commercially, with the remaining volumes burned as low value fuel [4].  
49 Nevertheless, lignin has a significant potential as a feedstock for the sustainable production of fuels  
50 and bulk chemicals, and indeed lignin can be regarded as the major aromatic resource of the bio-  
51 based economy [1].

52 Various pathways have been explored for the conversion of lignin-rich residual material for fuels or  
53 phenols [1,5-7]. Among them, thermochemical conversion by fast pyrolysis is one of the central  
54 techniques, but the resulting “oil” has a high O/C and low of H/C ratio. These bio-oils are very acidic  
55 and corrosive and often chemically unstable, making it necessary to further upgrade them to  
56 produce motor fuels and chemicals to be used in the petrochemical industry [8-10]. In comparison to  
57 fast pyrolysis, solvolysis provides the advantages of milder conditions and a single phase  
58 environment due to the miscibility of the organic products in the (supercritical) solvent. Further  
59 advantages of solvolysis performed in polar solvents such as ethanol or iso-propanol [11] over fast  
60 pyrolysis are a less oxygenated oil fraction and almost no solid residue (< 5%) [12,13]. A promising  
61 and relatively new lignin conversion methodology involves the use of a hydrogen donor solvent  
62 instead of molecular hydrogen [14]. A well-known hydrogen donor is formic acid (FA), which is  
63 converted *in situ*, either thermally or catalytically, to molecular hydrogen and CO/CO<sub>2</sub>. Commonly  
64 used solvents are alcohols (methanol, ethanol) and water, the latter being a preferred system for  
65 biofuel conversion since it is a “green” solvent.

66  
67 With temperatures typically of 350-400°C and reaction times of typically 8-16 hours, lignin from  
68 spruce, pine, birch and aspen wood has been converted to a chemically stable bio-oil through a  
69 solvolysis process using formic acid as hydrogen donor. The molar H/C ratio of the product was  
70 between 1.3 and 1.8, and the O/C ratio between 0.05 and 0.1, indicative of a substantial reduction in

71 the oxygen content compared with the **fast** pyrolysis process [2,14,15]. However, in order to make  
72 this bio-oil fuel competitive with fuels and chemicals obtained from petroleum, some important  
73 process parameters need to be improved: i) shorter reaction times, ii) lower reaction temperatures  
74 and iii) the reduction of low-value side streams i.e. gas and solid residues.

75  
76 One possibility to address these challenges is the use of catalysts in the process. Catalytic  
77 hydrotreatment of lignin has already been explored extensively and involves the reaction of lignin in  
78 the presence of a (heterogeneous) catalyst with molecular hydrogen at elevated temperatures.  
79 Several catalytic systems have been evaluated both with model compounds and lignin [5,6]. Catalysts  
80 such as Co-Mo/Al<sub>2</sub>O<sub>3</sub> and Ni-Mo/Al<sub>2</sub>O<sub>3</sub> and noble metals on different supports, Rh/C, Rh/Al<sub>2</sub>O<sub>3</sub>, Pd/C,  
81 Rh/ZrO<sub>2</sub>, Ru/C [1] have extensively been evaluated for this purpose. Although very effective when  
82 using model compounds, only low levels of lignin conversion is achieved in such lignin based systems  
83 [5]. Recent research by Ligouri and Barth showed that the reaction time and temperature can be  
84 reduced dramatically when using heterogeneous (Pd/C) catalyst together with Nafion SAC-13 as solid  
85 superacid in a formic acid/water media (2011) [16]. The Pd/C catalyst increases the hydrogenation  
86 rate, while the Nafion SAC-13, a Brønsted acid, activates the lignin aryl ether sites (de-  
87 polymerization) and promotes their hydrogenolysis to phenols[17]. The lignin was converted at a  
88 reaction temperature of 300°C and a reaction time of 2 h, and high conversions into oil were  
89 achieved. Nonetheless, the use of two types of catalyst presents some drawbacks from an industrial  
90 and economical point of view. In this perspective, the use of a bifunctional catalyst where a cheap acid  
91 support is used could have the potential to improve the industrial and economic performance  
92 without lowering the lignin conversion values. **Alumina could be an adequate alternative, although**  
93 **the role of its Lewis acidity in the lignin de-polymerization and re-polymerization needs investigation.**

94 In this study, several noble metals supported on alumina, Ru/Al<sub>2</sub>O<sub>3</sub>, Rh/Al<sub>2</sub>O<sub>3</sub> and Pd/Al<sub>2</sub>O<sub>3</sub> are  
95 investigated as bifunctional catalyst in a formic acid/water media for the simultaneous de-  
96 polymerization and hydrodeoxygenation of three different types of lignins. The conversion of lignin  
97 to oil and solids (coke) and the effect of the **alumina as a support with Lewis acid properties** are  
98 investigated at different temperatures (340-380°C) and reaction times (2-6 h), in terms of bulk yields  
99 and chemical composition of the products.

100

## 101 2. Materials and Methods

### 102 2.1 Chemicals

103 N,O-Bis(trimethylsilyl)trifluoroacetamide (BSTFA) with trimethylchlorosilane (TMCS) and pyridine  
104 (>99.5 %) was purchased from Fluka and used as bought. Pentane (>99%), formic acid (>98%),  
105 tetrahydrofuran (>99.9%) and ethyl acetate (99.8%) were purchase from Sigma Aldrich and used as  
106 bought.

### 107 2.2 Catalysts

108 Ruthenium on alumina (5 wt%), Rhodium on alumina (5wt%) and Palladium on alumina (10 wt%)  
109 were obtained from Sigma Aldrich, and gamma-alumina (97 wt%) was obtained from Strem  
110 Chemicals Inc. These were dried at 80°C for 24 h prior to use.

### 111 2.3. Acidity measurements (DRIFT and NH<sub>3</sub>-TPD)

112 Temperature-programmed desorption of ammonia, NH<sub>3</sub>-TPD, was performed to determine the total  
113 acidity of the samples. The measurements were carried out in chemisorption analyzer AutoChem II  
114 equipped with a thermal conductivity detector (Micromeritics, USA). The samples (50 mg) were  
115 flushed with helium at 650°C for 30 min, then cooled down to 40°C and loaded with ammonia for 30  
116 min. Complete removal of physically adsorbed ammonia was carried out by purging the saturated  
117 samples with helium at 100°C until no further desorption was recorded. Under constant flow of  
118 helium, the samples were heated up from 100 to 650°C at a heating rate of 10°C/min, and the  
119 release of ammonia was recorded. The total acidity was determined by using calibration data.

120 Diffuse reflectance infrared Fourier transform, DRIFT, was used to distinguish Lewis and Brønsted  
121 acid sites of noble-metal containing catalysts and  $\gamma$ -Al<sub>2</sub>O<sub>3</sub>. The analyses were done using a VERTEX 70  
122 spectrometer coupled with an external sample chamber that enables measurements under vacuum  
123 (Bruker, Germany). The samples were dried *in situ* under vacuum for 1 h at 250°C and later cooled  
124 down to 40°C in order to record the background spectra. The main measurement features were a  
125 spectral range from 1650 to 1350 cm<sup>-1</sup>, 200 scans, and a resolution of 4 cm<sup>-1</sup>. Initially, the catalyst  
126 was brought in direct contact with pyridine at 40°C for 15 min. Analysis where obtained by heating  
127 the sample up to 100, 200, or 300°C for 15 min.

### 128 2.4 Type of lignins

129 Low sulfonate alkali lignin (KL lignin) was purchase from Sigma-Aldrich. Lignin from Norway spruce  
130 from strong acid carbohydrate dissolution pre-treatment (AL) was received from Technical College of  
131 Bergen, and lignin from Norway spruce from weak acid and enzymatic hydrolysis biomass pre-

132 treatment (EL) was received from the Norwegian University of Life Science in Ås. The two latter  
133 lignins were ground and sieved (<500µm). All the lignins were dried at 80°C for 24 h prior to use.

## 134 **2.5 Experimental conditions**

### 135 **2.5.1 Experimental set-up**

136 A detailed description is given elsewhere by Kleinert and Barth (2008) [14]. Briefly summarised, lignin  
137 (2g), formic acid (3.075g), water (5g) and the catalyst (0.2g) were added to a stainless steel reactor  
138 (Parr 4742 non-stirred reactor, 25 ml volume). The amounts of reactants are based on previous  
139 experiments for maximising oil yields. The reactor was closed and heated in a Carbolite LHT oven to  
140 the desired conditions (340°C or 380°C) for a given reaction time (2 or 6 hours). The experimental  
141 conditions for all the experiments are summarized in Supplementary Material Table S1.

### 142 **2.5.2 Sample work-up**

143 After completed reaction time, the reactors were taken out of the oven and cooled in an air stream  
144 to ambient temperature. The amount of produced gases was determined by weighting the reactor  
145 before and after ventilating the gas. After opening the reaction container, the liquid reaction mixture  
146 was extracted with a solution of ethyl acetate: tetrahydrofuran (90:10) and the solid phase  
147 (unreacted lignin, reaction products and catalyst) were filtered. Two well-separated liquid phases  
148 were obtained (organic top phase and aqueous bottom phase). They were separated by decanting,  
149 and the pH and the weight of the aqueous phase was determined. The organic phase was dried over  
150 Na<sub>2</sub>SO<sub>4</sub> and concentrated at reduced pressure (ca. 250 mbar) at 40°C to yield a dark brown to black  
151 liquid. The yield was determined by weight. The solids were characterized by Fourier-Transformed  
152 Infrared Spectroscopy (FT-IR) and elemental analysis. The oil fraction was characterized by gas  
153 chromatography (GC-FID), gel permeation chromatography-size exclusion chromatography (GPC-SEC)  
154 and electrospray soft ionization mass spectroscopy (ESI-MS).

### 155 **2.6 GC-FID analysis**

156 The oil was silylated with BSTFA prior to the GC-FID analysis. Typically 3 mg of oil was dissolved in  
157 100 µL of pyridine and latter 100 µL of BSTFA with TMS was added. The samples were heated to 70°C  
158 for 20 min. After cooling the mixture was dissolved with pentane (3mg of oil/ml of pentane) and  
159 analysed by GC-FID.

160 The samples were analysed on a Thermo Finnigan TRACE GC Ultra with a FID- detector equipped with  
161 a chromatographic HP-ULTRA2 [(5%-phenyl-methylpolysiloxane), 25m, 0.200 ID column from Agilent  
162 Technologies. The following heating programme was applied: 30°C for one minute, and then heating

163 at 10°C/min up to 250°C. The injector temperature was 250°C, and the detector temperature was  
164 320°C. Identification of the peaks was made by comparison with retention times of authentic  
165 commercially available reference compounds that were also silylated prior to the analysis. The  
166 quantitative data was obtained using hexadecane as internal standard. Calibration curves were  
167 prepared for the following compounds: phenol, cresol, guaiacol, methylguaiacol, catechol,  
168 ethylcatechol, syringol, o-vanillin.

## 169 2.7 Elemental analysis

170 All samples were analysed for their elemental composition in the CHNS mode with a Vario EL III  
171 instrument using helium as carrier gas. The amount of oxygen was calculated by difference.

## 172 2.8 GPC-SEC

173 The sample (1 mg) was dissolved in 1 mL of THF. The solution (20 µL) was injected into a GPC-SEC  
174 system equipped with a PLgel 3µm Mini MIX-E column, and analysed at a flow rate of 0.5 ml/min of  
175 THF at 21.1°C, and the detection was performed with UV at 254 and 280 nm, as well as with RI. The  
176 set of columns was calibrated with a series of polystyrene standards covering a molecular-mass  
177 range of 162-2360 Da.

## 178 2.9 FT-IR

179 The FTIR spectra were recorded by applying the sample to an attenuated total reflectance (ATR)  
180 crystal. The main measurement features were a spectral range from 4000 to 400 cm<sup>-1</sup>, 16 scans, and  
181 a resolution of 4 cm<sup>-1</sup>.

## 182 2.10 ESI-MS

183 Each sample (120 µg/ml) was dissolved in methanol and analysed by full-scan mass spectrometry  
184 (m/z range from 100 to 1000 with 1 scan/s) on an Agilent 6420 Triple Quad LC/MS system (Agilent  
185 Technologies, Inc., Palo Alto, CA). Samples of 2 µL were injected by direct injection into the ESI-MS.  
186 Both positive and negative electrospray ionization was used to detect different compounds.

## 187 2.11 Gas phase GC

188 Gas phase GC analysis was performed on a GC-FID/TCD (HP 7890A) and a 30 m Porapak Q Molsieve  
189 column equipped with a FID front detector and a TCD back detector, which was controlled by an  
190 HPChem laboratory data system. The heating programme was as follows: Initial temperature was  
191 50°C for 22 min after which, the temperature was raised at a rate of 20°C/min up to 150°C. 15 min  
192 after reaching this temperature it was again raised at a rate of 50°C/min up to 220°C. This

193 temperature was held for 5 min. The injection port had a temperature of 250°C, the pressure was  
194 kept constant at 255 kPa and the FID was at 300°C.

## 195 **2.12 Energy dispersive X-ray analysis (EDXA)**

196 Compositional analysis of the reactor surface was carried out with an EDX spectrometer equipped  
197 with an SEM system (JEOL, JSM-5610LVS). The measurement duration of SEM-EDX analysis was set to  
198 300 s. The energies of the obtained EDX spectra were calibrated by Cu-L $\alpha$  and K $\alpha$  lines of a copper  
199 (99.96%) plate.

## 200 **3. Results**

### 201 **3.1 Acidity Results**

202 Acidity measurements on the Ru/Al<sub>2</sub>O<sub>3</sub>, Rh/Al<sub>2</sub>O<sub>3</sub>, Pd/Al<sub>2</sub>O<sub>3</sub> and  $\gamma$ -alumina were carried out to  
203 determine the type of acidity (Lewis or Brønsted), the acidity retention and total acidity of the  
204 samples. Table 1 shows the total acidity data recorded by NH<sub>3</sub>-TPD in the 100-650°C temperature  
205 range. The highest acidity was obtained for the  $\gamma$ -Al<sub>2</sub>O<sub>3</sub> (1.51 mmol NH<sub>3</sub>/g cat.), with significantly  
206 lower acidities for the supported catalysts (Rh/Al<sub>2</sub>O<sub>3</sub> > Ru/Al<sub>2</sub>O<sub>3</sub> > Pd/Al<sub>2</sub>O<sub>3</sub>).

207

208 Table 1: Total acidity, acidity retention and active acidity of  $\gamma$ -alumina, Rh/Al<sub>2</sub>O<sub>3</sub>, Ru/Al<sub>2</sub>O<sub>3</sub> and  
209 Pd/Al<sub>2</sub>O<sub>3</sub>.

210 a) Data obtained from NH<sub>3</sub>-TPD b) Data obtained from DRIFT

211

212 The DRIFT spectra (see Supplementary Material Figure S1) of all the catalysts show sharp IR bands at  
213 1445 and 1610 cm<sup>-1</sup>, that are assigned to Lewis acid sites [18]. IR bands assigned to Brønsted acid  
214 sites (1545 and 1638 cm<sup>-1</sup>) were not detected in any of the samples [18]. Based on the IR band at  
215 1445 cm<sup>-1</sup>, acidity retention was also calculated as [peak area (T) / peak area (100°C)] x 100 (Table 1).  
216 Increasing the temperature did not influence the Lewis acid-bound pyridine in Al<sub>2</sub>O<sub>3</sub> and Pd/Al<sub>2</sub>O<sub>3</sub>, as  
217 peak areas are not altered. In contrast, increased temperature causes pyridine desorption in  
218 Rh/Al<sub>2</sub>O<sub>3</sub> and Ru/Al<sub>2</sub>O<sub>3</sub> samples, which suggests that their acidity is rather weak. Given the reaction  
219 temperature, only the acidity obtained above 300°C could actively participate in the reaction, due to  
220 its capability to retain pyridine or similar molecules at the given reaction temperatures. Therefore  
221 the active acidity, define as the fraction of total acidity that actually plays a significant role in the  
222 reaction was calculated (active acidity (T) = acidity retention (T) x total acidity) and the results are  
223 shown in Table 1. The catalyst with the highest active acidity is  $\gamma$ - Al<sub>2</sub>O<sub>3</sub> followed by Pd/Al<sub>2</sub>O<sub>3</sub>,  
224 Rh/Al<sub>2</sub>O<sub>3</sub> and Ru/Al<sub>2</sub>O<sub>3</sub>.

225

## 226 **3.2 Influence of the reaction surface**

### 227 **3.2.1 Analysis of the reactor surface**



228 The composition of the reactor surface can affect the final results of our system. The reactor used is a  
229 T316 stainless steel Parr reactor. The metals present in the reactor surface could in principle catalyze  
230 the hydrodeoxygenation reactions and therefore affect the final product distribution [19].

231 Furthermore, when the reactor is used for repeated solvolysis reactions, alterations in the reactor  
232 surface are observed, and the metallic surface turns black. Previous experience in our group shows  
233 an improvement in the oil yields obtained after the reactor was submitted to 3-4 reaction cycles,  
234 suggesting that these alterations in the reactor surface are beneficial for the overall process.

235 To evaluate these changes and the possible metals that could have a catalytic effect in the reaction  
236 system, an EDXA analysis of the non-altered and the altered reactor surface was carried out. The  
237 results are shown in Table 2.

238

239 Table 2: Elemental composition of the altered and non-altered T316 stainless steel reactor surface

240

241 The composition of the non-altered surface is in accordance to the data provided by the producer,  
242 which confirms the suitability of this method to analyze the surface composition. When comparing  
243 both surfaces, several differences in the composition are observed. The content of Fe, Cr and Mn  
244 decreases significantly, while the O,C and Ni and Mo content increases.

### 245 **3.2.2 Effect of the reactor surface in the non-catalyzed and catalyzed system**

246 With the aim of evaluating the effect of the reactor surface, four experiments at a temperature of  
247 340°C and 6 hours were performed. Two of the experiments, NC-Q and NC-1, were carried out  
248 without the catalyst, with and without a quartz insert to prevent contact between the system and  
249 the reactor surface. Subsequently, the equivalent experiments were carried out using Ruthenium on  
250 alumina (Ru/Al<sub>2</sub>O<sub>3</sub>) as catalyst (Ru-Q and RU-1).

251 Table 3 shows the results for these experiments. When the contact between the system and the  
252 reactor surface is reduced by using the quartz insert, the oil yield decreases by 11 wt% and the solid  
253 yield increases by 13 wt%. However, when the analogous experiments are done in the presence of  
254 the Ru catalyst, no significant difference is observed. Actually, when using the quartz liner, the oil  
255 yield is slightly higher and the solid yield is slightly lower.

256

257 Table 3: Mass balance of the selected experiments at 340°C

258 **NC:** non-catalyzed experiment. **A:**  $\gamma$ -alumina (0.2 g). **Rh:** rhodium on alumina (0.2 g). **Ru:** ruthenium on alumina (0.2 g). **Pd:** palladium on  
259 alumina (0.2 g). **Q:** A quartz insert was used to suppress the effect of the reactor wall **a)** **Reaction conditions:** 340°C and 6 h. 2 g of acid  
260 hydrolysis lignin, 5.0 g of water and 3.075 g of formic acid.

261

### 262 **3.3 Screening of Rh (Rh/Al<sub>2</sub>O<sub>3</sub>), Ru (Ru/Al<sub>2</sub>O<sub>3</sub>) and Pd (Pd/Al<sub>2</sub>O<sub>3</sub>) on alumina**

#### 263 **3.3.1 Reproducibility and mass balance**

264 **Table 3** shows the yields as a function of the inputs for the first replicate of each system. The lignin  
265 mass balance accounts for the amount of solids and oil (g) divided by the amount of lignin  
266 introduced, while the water recovery percentage accounts for the ratio of water phase recovered (g.)  
267 with respect to the water phase introduced (g.). All the experiments show a total mass balance of  
268 nearly a 100%, only the gamma-alumina ( $\gamma$ -Al<sub>2</sub>O<sub>3</sub>) system has a value around 94,8%, which can be  
269 assigned to the low water recovery percentage.

270 **Table 3** shows that the solvolysis approach comprises of four major products: a gas phase, a solid  
271 phase, an aqueous liquid phase and an organic liquid phase (bio-oil). The amount of gas recovered  
272 after the reaction is very close to the values of the formic acid introduced, which supports that the  
273 main components of the gas phase are the decomposition products of the formic acid.

274 As mentioned above, the liquid phase obtained after the reaction can be divided into the clear water  
275 phase and the organic oil product. **The water phase recovered mostly accounts for slightly higher**  
276 **amounts than the one introduced (see Table 3), which suggests that the water does not act as a**  
277 **reactant, but rather a solvent in the reaction media. Some water-soluble organics and water**  
278 **produced in deoxygenation reactions [20,21] could account for the increased amounts of water**  
279 **recovered, and also for the mass loss in the quantified products relative to the lignin input.** The solid  
280 yield for the catalyzed systems is calculated after subtracting the amount of catalyst introduced. The  
281 sum of this value and the oil yield accounts for over 80 % of the lignin introduced for all experiments,  
282 and is even higher, 95 %, for the Ru catalyst. This supports that the solid and oil are the main  
283 products of the lignin de-polymerization and hydrodeoxygenation.

284 **Table 4** shows a summary of the results for the three different replicates carried out for each system,  
285 the average of the oil and solid yield for each system, and the standard deviation from the average  
286 values. It can be observed the Ru system shows the highest standard deviation in terms of oil yield  
287 (6.3 wt%) while the alumina system shows the highest standard deviation in terms of solid yield (4.3  
288 wt%).

289

290 **Table 4:** Average oil and solid yields for the selected replicates

291 **NC:** non-catalyzed experiment. **A:**  $\gamma$ -alumina (0.2 g). **Rh:** rhodium on alumina (0.2 g). **Ru:** ruthenium on alumina (0.2 g). **Pd:** palladium on  
292 alumina (0.2 g). **a) Reaction conditions:** 340°C and 6 h. 2 g of acid hydrolysis lignin, 5.0 g of water and 3.075 g of formic acid.

293

### 294 3.3.2 Effect of the catalyst on the oil and solid yields

295 From the results in **Table 4** we can clearly see the effect of the catalysts in our reaction system. For  
296 the non-catalyzed system the average oil yield accounts for  $61.6 \pm 3.0$  wt% and the solid for  $20.6 \pm$   
297  $3.4$  wt% of the lignin input. These results are comparable to the ones obtained in the gamma-alumina  
298 catalyzed system ( $62.8 \pm 3.9$  wt% oil yield and  $21.6 \pm 4.3$  wt% solid yield). However, when comparing  
299 these systems with the supported catalyst systems, Rh/  $\text{Al}_2\text{O}_3$ , Pd/  $\text{Al}_2\text{O}_3$ , Ru/  $\text{Al}_2\text{O}_3$ , a substantial  
300 increase in the oil yield together with a decrease in the solid yield is observed. The best result in  
301 terms of oil yield is obtained for the Ru catalyst with an increase of 29.9 wt%. Both the Pd and the Rh  
302 catalyst show comparable oil yield with  $82.9 \pm 2.2$  wt% and  $80.5 \pm 3.7$  wt% respectively. In terms of  
303 solid yield the best values are obtained for the Pd catalyst, where nearly no solid is found ( $2.7 \pm 0.3$   
304 wt%). In the case of the Ru and Rh systems, slightly higher amounts of solids are obtained, with an  
305 average of  $4.2 \pm 1.0$  wt% and  $4.6 \pm 0.5$  wt% respectively.

### 306 3.3.3 Oil phase composition

307 The main components in the oil have been quantitatively analyzed by GC-FID as the tri-methyl silyl  
308 (TMS) derivatives. The results of the quantification are summarized in **Table 5**. The **Ru-catalyzed**  
309 **system shows the higher abundance of highly hydrogenated and lower oxygenated compounds such**  
310 **as phenol (1.99 %) and cresol (4.27 %), followed by the Pd catalyst, the non-catalyzed system, the**  
311 **alumina catalyzed system and the Rh system. Less hydrogenated compounds such as catechol and**  
312 **ethyl-catechol are more abundant in the alumina system (3.15 and 3.24% respectively), followed by**  
313 **the palladium, non-catalyzed, ruthenium and Rh systems.**

314

315 **Table 5:** Quantification of the main oil components by GC-FID **and molecular weight distributions by**  
316 **GPC-SEC**

317

318 **NC:** non-catalyzed experiment. **A:**  $\gamma$ -alumina (0.2 g). **Rh:** rhodium on alumina (0.2 g). **Ru:** ruthenium on alumina (0.2 g). **Pd:** palladium on  
319 alumina (0.2 g). **a) Reaction conditions:** 340°C and 6 h. 2 g of acid hydrolysis lignin, 5.0 g of water and 3.075 g of formic acid. **b) Reaction**  
320 **conditions:** 380°C and 2 h. 2 g of acid hydrolysis lignin, 5.0 g of water and 3.075 g of formic acid.

321

322 Table 6 gives the elemental composition of the oil. The H/C ratio is highest when using the Pd, Rh and  
323  $\gamma$ -alumina catalyst, although comparable results are obtained for all the experiments. However when  
324 analyzing the O/C ratio, significant differences are observed. The Pd and Rh catalyzed oils clearly has  
325 the lowest O/C ratio (0.14), the Ru and the non-catalyzed systems have comparable values, and the  
326 highest value is obtained for the alumina catalyzed system.

327

328 **Table 6: Results of the elemental analysis of the lignin, oils and solids**

329 **NC:** non-catalyzed experiment. **A:**  $\gamma$ -alumina (0.2 g). **Rh:** rhodium on alumina (0.2 g). **Ru:** ruthenium on alumina (0.2 g). **Pd:** palladium on  
330 alumina (0.2 g). **AL:** acid hydrolysis lignin **a) Reaction conditions:** 340°C and 6 h. 2 g of acid hydrolysis lignin, 5.0 g of water and 3.075 g of  
331 formic acid. **b) Elemental analysis of the oil. c) Elemental analysis of the recovered solids**

332

333 According to the GPC-SEC analysis presented in Table 5, the  $\gamma$ -alumina catalyst generates the oil with  
334 the lowest average molecular weight (215 Da), followed by the Rh, Pd, non-catalyzed and Ru  
335 systems. When analyzing the GPC-SEC spectras in Figure 1, more information about the product  
336 distribution of the oils can be obtained. The shape of the peaks are narrower, nearly symmetric for  
337 the Rh and the non-catalyzed oils, but in the case of the Al and Pd the right side of the curve is less  
338 steep implying a higher concentration of lower molecular weight compounds.

339 Figure 1. GPC spectras of the oils for the NC-1, A-1, Ru-1, Rh-1 and Pd-1 experiments. Analytical  
340 conditions are given in section 2.8.

341 The ESI-MS spectra show a clear difference in the composition of the oils (see Supplementary  
342 Material Figure S2a-e). The alumina system shows the narrowest product distribution, with high  
343 intensity peaks in the low molecular range, 100-300 Da. The Ru, Pd and Rh catalyst show high  
344 intensity peaks in both low molecular range (100-300 Da) and medium molecular range (300-600 Da)  
345 which could explain the lower proportion of quantified compounds obtained by the GC-FID. In the  
346 case of the non-catalyzed system, a very wide product distribution is observed, with a high  
347 concentration of medium molecular range products (300-600 Da) and intense peaks even in the high  
348 molecular mass range.

349 Overall, the more hydrodeoxygenated oils are obtained in the case of the supported systems, as  
350 shown in the GC-FID and elemental analysis data, while lower average-molecular-weight oils are  
351 obtained in the  $\gamma$ -alumina and Pd systems. The reason for these results will be further discussed in  
352 section 4.

### 3.3.4 Solid phase composition

353  
354 The amount of solid phase obtained in the Ru, Rh and Pd catalyst was insignificant, preventing any  
355 analysis. However, higher amounts of solid were recovered in the non-catalyzed and  $\gamma$ -alumina  
356 catalyzed systems. In **Figure 2**, the FT-IR spectras of the AL lignin, non-catalyzed solid phase products  
357 and gamma alumina solid phase products are compared with the aim of gaining insight into the  
358 nature of the solids, and the re-polymerization mechanism.

359 Two main observations can be **made**: i) the proportion of functional groups in the Al solids is much  
360 lower than in the non-catalyzed solid and the lignin; ii) there are significant differences between the  
361 solid obtained in the Al and the non-catalyzed system. It can be observed that the OH- stretching  
362 signal is broad ( $3500\text{-}3400\text{ cm}^{-1}$ ) for both non-catalyzed and lignin spectra, while a much narrow  
363 signal is found in the alumina solid, suggesting that a lower abundance of intramolecular H-bonding  
364 in the latter. In addition, the CH- stretching signal for methyl and methylene peak ( $2940\text{-}2930\text{ cm}^{-1}$ ) is  
365 not found in the Al experiment, which suggests an absence of these functional groups compared to  
366 the non-catalyzed system and the lignin. The same trend is seen for the carbonyl function **above**  
367  $1700\text{ cm}^{-1}$ , it is quite intense in the lignin **with a peak at  $1705\text{ cm}^{-1}$  which is typical for carboxylic acid**.  
368 **In the non-catalyzed oil there is a less intense peak at  $1788\text{ cm}^{-1}$ , indicating ester groups** and the  
369 carbonyl peak is inexistent in the alumina **catalyzed solids**. Some of the aromatic nature is retain in  
370 the alumina solid, as seen when analyzing the  $1605\text{-}1600$ ,  $1515\text{-}1505$  and the  $1430\text{-}1425\text{ cm}^{-1}$   
371 ranges, although this peaks are less intense than in the lignin and non-catalyzed solid [22]. The  
372 guaiacyl pattern is present in the lignin spectra, and the syringyl pattern in both the lignin and the  
373 non-catalyzed system. However, **both** the lignin and the alumina **catalyzed solids** spectra **has a**  
374 strong peak at around  $1065\text{ cm}^{-1}$ , which can be assign to the C-O ether stretching (all band indexing is  
375 summarized in the Supplementary Material Table S2).

376

377 **Figure 2**. FT-IR spectra for the AL lignin and the solids obtained in the **A-1 and NC-1 experiments**. For  
378 **experimental conditions, see Table 1**.

379

380 The results of the elemental analysis of the lignin and solid phases confirme the differences between  
381 these solids (**Table 6**). The non-catalyzed solids have a high content of carbon (73.63 wt%), followed  
382 by the lignin (61.27 wt%) and the alumina solids (42.6 wt%), while the content in O is higher for the  
383 alumina (53.82 wt%) and less than half for the non-catalyzed system (21.18 wt%).

### 384 3.3.5 Gas phase

385 The gas phase was analyzed for the non-catalyzed and the supported catalyzed systems, and the  
386 concentration of CO<sub>2</sub>, CO, H<sub>2</sub> and some light alkanes (methane, ethane, propane and butane) were  
387 measured, see Table 7.

388

389 **Table 7:** Composition of the gas phase for the selected experiments

390 **NC:** non-catalyzed experiment. **A:**  $\gamma$ -alumina (0.2 g). **Rh:** rhodium on alumina (0.2 g). **Ru:** ruthenium on alumina (0.2 g). **Pd:** palladium on  
391 alumina (0.2 g). **a) Reaction conditions:** 340°C and 6 h. 2 g of acid hydrolysis lignin, 5.0 g of water and 3.075 g of formic acid.

392

393 No water was **determined** in the gas phase due to the inability to measure this by the selected  
394 method. Nevertheless, the analysis of the mass balance suggests that the water produced through  
395 the decomposition of the formic acid and the water-gas-shift-reaction (WGS) mainly condenses in the  
396 liquid water phase.

397 The main gas product in all cases is CO<sub>2</sub>, produced mainly by the decomposition of the formic acid  
398 but also through decarboxylation and gasification reactions of the lignin and its monomers. The  
399 component with the second highest concentration is H<sub>2</sub>, which can have a strong influence in the  
400 hydrogenation rate of the depolymerized lignin monomers. The hydrogen seen in these  
401 measurements does not account for all the hydrogen produced from decomposition of formic acid in  
402 the course of the reaction, since considerable quantities are used for the hydrogenation of the  
403 monomers, especially in the catalytic systems, as suggested by the higher oil yields (Table 3).

404 When comparing the different systems the following conclusion can be stated: i) the catalytic  
405 systems enhance the production of CO<sub>2</sub> (especially Pd and Rh), ii) the amount of hydrogen is higher in  
406 the Ru system, iii) the amount of CO is lower in all the catalytic systems (especially Ru) and **the**  
407 **concentration of light hydrocarbons which are Fischer-Tropsch type reaction products** are higher  
408 when using the Pd and Rh.

### 409 3.4 Influence of the type of lignin

410 Three different types of lignins were tested to evaluate the influence of the lignin type in the non-  
411 catalyzed and catalyzed systems. To ensure sufficient oil yields in all systems, the experiments were  
412 carried out at 380°C and 2 hours reaction time. In total nine experiments were done, one non-

413 catalyzed and two catalyzed (Rh and Ru) experiments for each lignin. The results obtained are  
414 summarized in [Table 8](#).

415

416 [Table 8: Mass balance and aqueous pH of experiment with different lignins at 380°C](#)

417 **NC:** non-catalyzed experiment. **A:**  $\gamma$ -alumina (0.2 g). **Rh:** rhodium on alumina (0.2 g). **Ru:** ruthenium on alumina (0.2 g). **Pd:** palladium on  
418 alumina (0.2 g). **AL:** acid hydrolysis lignin. **KL:** kraft lignin. **EL:** enzymatic hydrolysis lignin **a)** **Reaction conditions:** 380°C and 2 h. 2 g of acid  
419 hydrolysis lignin, 5.0 g of water and 3.075 g of formic acid.

420

421 The most obvious difference between the three lignins is in the pH of the recovered water phase.  
422 While the KL lignin, which is a low sulfonate lignin derived from a kraft pretreatment process, yields a  
423 water phase with a basic pH, the EL and the AL lignin yield acidic water phases. This is highly  
424 correlated with the performance of the catalyst in the different lignin systems. For the KL lignin, with  
425 final water phases pH from 8-9, there is no significant difference between the non-catalyzed and  
426 catalyzed systems. The best results are obtained for the Rh catalyst, with an oil yield of 52.3 wt% and  
427 a solid yield of 9.99 wt%, but these differences are not significant, and even lower oil yields are  
428 obtained in the case of the Ru catalyst. In contrast, significant differences in the oil yield values are  
429 observed for those lignins with a final water phase pH lower than 7. Here, the oil yield is increased  
430 and the solid yield decreased when using the catalysts. In the case of the acid lignin there is an  
431 increased of the oil yield in 30 wt% when using the Ru catalyst, while in the enzymatic lignin we  
432 obtained an increase of 19 wt%. In both cases the solid yield were reduced.

433 To further evaluate the role of the alumina support in the AL and EL lignin, **three** additional  
434 experiments using only the  $\gamma$ -alumina as catalyst where carried out at a temperature of 380°C and 2  
435 hour reaction time ([experiments A-4, A-KL and A-EL](#)). These results are compared with the non-  
436 catalyzed and Ru catalyzed results in [Table 8](#). For both lignins, at this reaction conditions, there is  
437 moderate increase in the oil yield when using the **alumina compared to the non-catalyzed system,**  
438 **with** a 3.4 wt% **increase** for the AL lignin and a 13.7 wt% **increase** for the EL lignin.

439 To further confirm the effect of the alumina catalyst in the AL lignin, the oils obtained were  
440 submitted to [GPC-SEC](#) and ESI-MS analysis (see Supplementary Material Figures [S3a-c](#)). As shown in  
441 section 3.3.3, **the average molecular weight of the oil is lower in the case of the alumina catalyzed**  
442 **experiment than in the case of the non-catalyzed system** ([Table 5](#)). Furthermore, when analyzing the  
443 ESI-MS results, it can be observed that the Ru and alumina oil spectrograms show a narrower

444 product distribution of the oils, mostly below the 500 Da, while in the non-catalyzed experiments the  
445 product distribution goes up to over 800 Da.

446 Another aspect that can be evaluated in these results is the nature of the solids when using the  
447 supported catalysts. In the case of the EL lignin, enough solids are recovered to analyze the non-  
448 catalyzed and the Ru supported catalyzed solid phase. In **Figure 3** FT-IR spectrograms of the solids  
449 obtained in the Ru and non-catalyzed system are compared with the FT-IR spectra of the EL lignin.  
450 We can clearly see that the Ru solids shows the same reduced OH stretching peak, the lack of the  
451 methylene and methyl peak, the low intensity peaks in the aromatic region and the strong ether peak  
452 that **appeared in** the alumina solids FT-IR spectra in section 3.3.4. The non-catalyzed solids also show  
453 comparable spectra to the solids analyzed **previously** (see **Figure 2**).

454

455 **Figure 3.** FT-IR spectras for the EL lignin and the solids obtained in the **Ru-EL and NC-EL experiments**

456

### 457 **3.5 Influence of the hydrogen partial pressure**

458

459 **Table 9:** Gas, oil and solid yield for the high pressure and low pressure (LP) and **reduced catalyst**  
460 **loading (LC)** experiments

461 **NC:** non-catalyzed experiment. **Ru:** ruthenium on alumina (0.2 g). **LP:** low pressure. **LC:** low catalyst content. **a) Reaction conditions:** 340°C  
462 and 6 h. 2 g of acid hydrolysis lignin, 5.0 g of water and 3.075 g of formic acid. **b) Reaction conditions:** 340°C and 6 h. 1 g of acid hydrolysis  
463 lignin, 2.5 g of water and 1.5375 g of formic acid and 0,1 g of catalyst. **c) 0.1 g of catalyst**

464

465 To evaluate the influence of the total reaction pressure of the system in the final oil and solid yield  
466 two extra experiments were carried out, one without catalyst and one with the Ru/Al<sub>2</sub>O<sub>3</sub> catalyst.  
467 The proportions of the reactants were held constant, but the amount of each reactant was reduced  
468 to half for the **NC-LP** and the **Ru-LP** experiments. A lower amount of reactant, specially a lower  
469 amount of formic acid, will generate **less** of gases when the reactor is heated. Since the reactor  
470 volume is constant, a lower total pressure **will result**, for the same temperature, **in** a lower hydrogen  
471 partial pressure.

472 **In Table 9** we compare the results of the low pressure experiments with their higher pressure  
473 counterparts. For the non-catalyzed experiments, **with reduced** pressure, the oil yield is decreased to



474 nearly the half, from 58.2 wt% to 29.9 wt%. The solid yields is correspondingly higher, increasing  
475 from 22.4 wt% to 44.9 wt%. However when the supported Ru catalyst is used this effect is partially  
476 neutralized. The oil yield is lower, but the decrease is less than in previous case, from 90.0 wt% to  
477 73.7 wt%. In the case of the solid yield, the increase is not significant, from 5.1 wt% to 6.6 wt%.

478 Another relevant result is the amount of gas obtained in the low-pressure experiments. Both for the  
479 NC-LP and the Ru-LP the gas percentage recovered is 3% higher than for their high pressure  
480 counterparts. This increase is observed together with a reduction in the values of the lignin mass  
481 balance percentage, suggesting that more lignin is gasified at these conditions.

### 482 3.6 Influence of the catalyst concentration

483 The amount of catalyst in the Ru system was reduced to 5 wt. % on lignin (Ru-LC) to evaluate the  
484 effect of the catalyst concentration. Even when the amount of catalyst was reduced to the half, the  
485 oil and solid yield does not vary significantly (Table 9). This suggests that the catalyst concentration  
486 could be reduced to 5 wt% on lignin without inducing major changes in the catalyst efficiencies.

## 487 4. Discussion

488 Replicate experiments in Table 4 show low standard deviation values, from 0.3 to 6% (n=3) for the oil  
489 and solid yields, which support that the reactions and workup are reproducible. The deviations that  
490 are observed can be caused by inhomogeneity in the lignins, evaporation of volatile compounds and  
491 experimental errors during the work-up procedure. The consistency of the reaction process and  
492 work-up procedure is further confirmed by mass balances shown in Table 3, with a total mass  
493 recovery above 95 wt% for all the cases, and higher than 98 wt % for the supported-catalyzed  
494 systems.

495 The effect of the selected catalysts (Ru/Al<sub>2</sub>O<sub>3</sub>, Rh/ Al<sub>2</sub>O<sub>3</sub> and Pd/ Al<sub>2</sub>O<sub>3</sub>) is positive for all the  
496 experimental conditions tested, as described in section 3.3.2. This could be due to kinetic control of  
497 the lignin degradation mechanism by the catalysts. Gasson and Forchheim [22,23] suggest that the  
498 primary reaction in lignin solvolysis is a fast de-polymerization step, followed by competing reactions  
499 giving hydrodeoxygenation or repolymerisation of the de-polymerized monomers. The apparent  
500 activation energy values obtained for this kinetic model show that the probability of re-  
501 polymerisation of the lignin monomers is reduced when the monomers are hydrodeoxygenated  
502 and/or alkylated (see the simplified reaction scheme in Figure 4).

503

504 Figure 4. Simplified reaction scheme of lignin degradation

505

506 This effect is further confirmed by the results described in section 3.2.2, section 3.3.3 and section 3.5.  
507 Section 3.2.2 showed that the presence of a metallic reaction surface containing among other metals  
508 Ni and Mo, can increase the oil yield and reduce the solid yield. These metals are well known  
509 catalysts for hydrodeoxygenating reactions [19], and can also provide the kinetic enhancement  
510 discussed above. Nevertheless, the quantitative results indicate that the activity of the metallic  
511 reaction surface is significantly lower than the activity of the Ru/Al<sub>2</sub>O<sub>3</sub> catalyst. Section 3.3.3 shows  
512 how the Ru, Rh and Pd systems have the highest H/C and lower O/C ratios in the oil phase products  
513 (Table 6) and the Ru and Pd systems the higher concentrations of highly hydrodeoxygenated  
514 compounds (Table 5). Finally, the results in section 3.5 also confirm this kinetic enhancement. The  
515 lower hydrogen partial pressure of the system lowers the hydrogenation rate, which significantly  
516 affects the oil and solid yield in the un-catalyzed system, while the Ru system is not as strongly  
517 affected. The oil yield is reduced to half in the case of the un-catalyzed system as opposed to only 17  
518 wt % reduction in the case of the Ru system, and the solid yield is doubled in the un-catalyzed system  
519 while it remains nearly stable for the Ru system. All this suggests that the Ru, Pd and Rh active  
520 phases will catalyze the hydrodeoxygenation reactions (see Figure 4), increasing the oil yield and  
521 reducing the solid yield.

522 Another point for evaluation is to what degree the bifunctionality of the catalyst is important. The  
523 role of the hydrogenating active site (Ru, Rh and Pd) has already been discussed, but the support  
524 materials may also play an important role in the lignin degradation mechanism. Previous work  
525 suggests that acid heterogeneous catalysts are able to catalyze the cleavage of ether bonds and  
526 cause de-polymerization of lignin[17,24], the polymerization of alcohols to ethers (re-polymerization)  
527 [25,26] and the deoxygenation of hydroxyl and methoxy aromatics [19,20]. Therefore an effect of the  
528 alumina support due to its acid nature could be expected. The results given in Table 4 show that  
529 alumina alone had no significant effect on the oil and solid yields, which may be due to the ability of  
530 alumina to catalyze both the de-polymerization and re-polymerization reactions. However, the  
531 composition of the oil shows a clear difference between the non-catalyzed and alumina catalyzed  
532 systems.

533 Table 5 indicates that the lowest values of average molecular weight are obtained for the oils from  
534 the  $\gamma$ -alumina and Pd systems. The ESI-MS analyses show that the  $\gamma$ -alumina has the highest  
535 concentration of low molecular weight compounds, followed by the Pd, Ru and Rh systems. The un-  
536 catalyzed system is the only one that shows high concentration of high molecular weight compounds.  
537 These results are in agreement with the acidity measurement in section 3.1. The  $\gamma$ -alumina sample

538 shows the highest stable acidity and consequently the oil obtained is the one with the lowest average  
539 molecular weight (215 Da). On the other hand, the oils in the noble metal containing catalysts have  
540 significantly higher average molecular weight in the following order: Pd/Al<sub>2</sub>O<sub>3</sub> (323 Da) < Rh/Al<sub>2</sub>O<sub>3</sub>  
541 (344 Da) < Ru/Al<sub>2</sub>O<sub>3</sub> (397 Da). Since this order is inversely proportional to the active acidity of the  
542 catalysts, we can conclude that stable -strong Lewis acid sites play an important role in the de-  
543 polymerization of lignin into monomers.

544 The acid alumina support could also be able to catalyze the re-polymerization of the lignin  
545 monomers, which can be confirmed by comparing the FT-IR spectra for the AL lignin, the non-  
546 catalyzed and the alumina system. As described in section 3.3.4, the solid phase from the  $\gamma$ -alumina  
547 system has limited or no presence of methylene and carbonyl functionalities, very low concentration  
548 of intramolecular H-bonding of the hydroxyl groups, low intensity of aromatic bands and quite  
549 intense ether functionalities. In addition to this, the elemental composition data (Table 6) show that  
550 the solid phase has a high O/C ratio, which suggests that the O atoms have been retained in poly-  
551 phenolic or aryl ether dominated solids. On the other hand, the lack of ether functionalities and low  
552 O/C ratio in the un-catalyzed system suggest a more graphite like structure of the solid phase for this  
553 system. We can conclude that the alumina support directs the reactions towards an aryl ether type  
554 structure through acid-catalyzed condensation reactions of the hydroxyl groups present in the  
555 depolymerized lignin monomers. The same comparison was done for reactions with EL lignin, where  
556 solids from the Ru and the non-catalyzed system were compared. In Figure 3 the most intense IR  
557 peak for the Ru solid also corresponds to C-O stretching, again indicating a predominance of ether  
558 moieties in the solid products.

559 The importance of the acidity of the reaction system for the final oil and solid yield can also be  
560 evaluated by comparing experiments with different pH values in the reaction medium. As shown in  
561 section 3.4, when the recovered water phase pH is >7 (KL lignin), no significant effect of the catalyst  
562 on the oil or solid yield is observed. There are two possible explanations for this observation; either  
563 the acid sites of the solid are deactivated, or the influence of the basicity of the lignin is just through  
564 the pH of the reaction mixture. The increased oil yields obtained from the acidic AL and EL lignins in  
565 the catalyzed systems suggest that the latter mechanism is the main reason for the lack of effect of  
566 the catalyst. Furthermore, if the  $\gamma$ -alumina system is compared with the non-catalyzed system, we  
567 can clearly see that the presence of alumina at 380°C and 2 h increases the amount of oil in acidic  
568 reaction media (marginally significant increase of 3.4 wt% for the A-4 experiment and a significant  
569 increase of 13.7 wt% for the A-EL experiment). This effect is higher for the EL lignin, which might be  
570 due to the higher pH of the reaction system. In the AL lignin, this increase is not so significant, but  
571 the GPC-SEC (Table 5) and the ESI-MS analysis confirms the higher amount of low molecular weight

572 compounds in the alumina system. All this implies that the properties of the selected lignin are a key  
573 factor when selecting the most efficient catalyst.

574 Finally, the effect of the catalysts in the composition of the gas phase should also be mentioned. The  
575 complexity of the reaction mechanisms producing the gas phase makes it complicated to analyze the  
576 reasons behind the disparity in the concentration of the components. It is clear that the lower CO  
577 values of the catalyzed systems (see section 3.3.5), can be caused by on the one hand, the  
578 displacement of the WGS equilibria towards the production of H<sub>2</sub>, predominant in the Ru catalyst,  
579 and on the other hand to the **Fischer-Tropsch type reactions** to low molecular weight hydrocarbons  
580 like methane, mainly in the Rh and Pd catalyst. The first mechanism is supported by the observation  
581 that higher H<sub>2</sub> amounts are found in the Ru system even though higher quantities of hydrogen are  
582 incorporated into the liquid products in the course of the reaction. The later mechanism is based on  
583 the observation that higher amounts of volatile alkanes are present in the Pd and Rh systems.  
584 Together, this indicates an effect of the catalyst in the final composition of the gas phase. In any case,  
585 the higher amount of hydrogen in the Ru system could be a reason for the highest oil yields obtained  
586 in this system.

## 587 **5. Conclusion**

588 The simultaneous catalytic de-polymerization and hydrodeoxygenation of KL, EL and AL lignings was  
589 carried out in a formic acid/water media and their results were compared with the non-catalyzed  
590 and a gamma-alumina support catalyzed system. Three bifunctional catalysts were screened, Rh, Pd  
591 and Ru on alumina, and evaluated in terms of the conversion of the lignin to oil and solids. A central  
592 focus of this paper was to identify the role of the alumina support and to evaluate its effect on the  
593 process. As a summary, the following conclusions can be made:

- 594 • The effect of the supported catalyst (Rh/Al<sub>2</sub>O<sub>3</sub>, Ru/Al<sub>2</sub>O<sub>3</sub>, Pd/Al<sub>2</sub>O<sub>3</sub>) is positive **with regard to**  
595 **an increase on oil yield and a decrease on solid yield.** The best result in terms of oil yield is  
596 **for the Ru system, while the most effective one for the reduction of the solid yield was the**  
597 **Pd system.**
- 598 • **When analyzing the composition of the oils, 8 major components are identified and**  
599 **quantified: phenol, cresol, guaiacol, methyl guaiacol, catechol, ethylcatechol, syringol and o-**  
600 **vanillin. Ru shows the highest amount of highly hydrodeoxygenated monomers, followed by**  
601 **the Pd catalysts. However, when analyzing the average elemental composition of the oils, Pd**  
602 **and Rh show lower O/C and higher H/C ratios.**
- 603 • **The alumina support plays a vital role in the de-polymerization of lignin. This has been**  
604 **proved by analyzing the yields and composition of the oil and by changing the type of lignin**

- 605 and consequently the pH of the reaction media. The presence of temperature-stable Lewis  
606 acid sites seems to increase the amount of low molecular weight compounds in the oils.
- 607 • The alumina support plays also a role in the re-polymerization of the lignin monomers. The  
608 elemental and FTIR analysis of the solids suggest an alternative re-polymerization mechanism  
609 when the alumina support is present in the system.
  - 610 • The type of lignin is a key factor when analyzing the effect of the selected catalyst. Only  
611 lignins that provide acid reaction media are suitable for this type of bifunctional catalysts.
  - 612 • The pressure has a strong influence in the final oil and solid yield. Under reduced pressure  
613 conditions, the oil yield is reduced while the solid yield is increased. This effect is partially  
614 neutralized when using a catalyst. In both cases the amount of lignin gasified increases.
  - 615 • The reactor surface has a positive effect on the oil and solid yield. This is due to mainly its Ni  
616 and Mo content, which can catalyze hydrodeoxygenation reactions.
  - 617 • The catalyst also affects the decomposition of the formic acid into molecular H<sub>2</sub> and CO/CO<sub>2</sub>.  
618 The Ru catalyst is able to induce a higher production of H<sub>2</sub>, while the Rh and Pd catalyst are  
619 responsible for a higher production of low molecular weight compounds.

620

621 Acknowledgements

622 We gratefully acknowledge financial support from the Lignoref project group, including The Research  
623 Council of Norway (grant no. 190965/S60), Statoil ASA, Borregaard AS, Allskog BA, Cambi AS, Xynergo  
624 AS/Norske Skog, Hafslund ASA and Weyland AS.

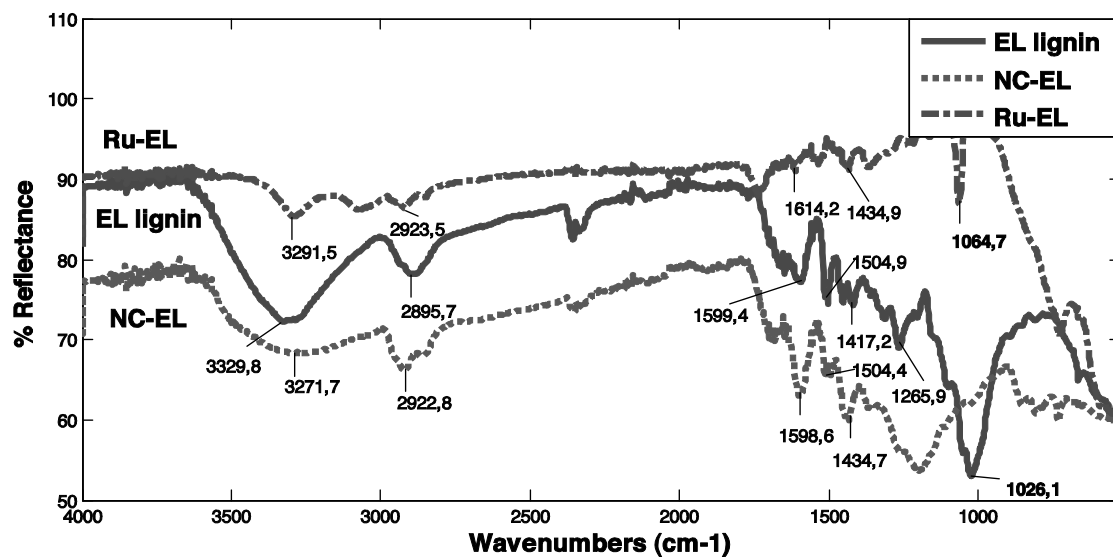
625

## 626 References

- 627  
628  
629 [1] J. Zakzeski, P.C.A. Bruijninx, A.L. Jongerius and B.M. Weckhuysen, *Chemical Reviews*, 110,  
630 (2010) 3552.  
631 [2] M. Kleinert, J.R. Gasson and T. Barth, *Journal of Analytical and Applied Pyrolysis*, 85, (2009)  
632 108.  
633 [3] A. Limayem and S.C. Ricke, *Progress in Energy and Combustion Science*, 38, (2012) 449.  
634 [4] R.J.A. Gosselink, E. de Jong, B. Guran and A. Abächerli, *Industrial Crops and Products*, 20,  
635 (2004) 121.  
636 [5] Q. Bu, H. Lei, A.H. Zacher, L. Wang, S. Ren, J. Liang, Y. Wei, Y. Liu, J. Tang, Q. Zhang and R.  
637 Ruan, *Bioresource Technology*, 124, (2012) 470.  
638 [6] A.L. Jongerius, P.C.A. Bruijninx and B.M. Weckhuysen, *Green Chemistry*, 15, (2013) 3049.  
639 [7] B. Li, W. Lv, Q. Zhang, T. Wang and L. Ma, *Journal of Analytical and Applied Pyrolysis*, 108,  
640 (2014) 295.  
641 [8] A.V. Bridgwater, *Chemical Engineering Journal*, 91, (2003) 87.  
642 [9] S. Czernik and A.V. Bridgwater, *Energy & Fuels*, 18, (2004) 590.  
643 [10] D.C. Elliott, *Energy & Fuels*, 21, (2007) 1792.  
644 [11] N.P. Vasilakos and D.M. Austgen, *Industrial & Engineering Chemistry Process Design and*  
645 *Development*, 24, (1985) 304.  
646 [12] E. Dorrestijn, M. Kranenburg, D. Poinsoot and P. Mulder, in *Holzforschung*, 1999, p. 611.  
647 [13] D. Mohan, C.U. Pittman and P.H. Steele, *Energy & Fuels*, 20, (2006) 848.  
648 [14] M. Kleinert and T. Barth, *Energy & Fuels*, 22, (2008) 1371.  
649 [15] M. Kleinert and T. Barth, *Chemical Engineering & Technology*, 31, (2008) 736.  
650 [16] L. Liguori and T. Barth, *Journal of Analytical and Applied Pyrolysis*, 92, (2011) 477.  
651 [17] C. Zhao, Y. Kou, A.A. Lemonidou, X. Li and J.A. Lercher, *Chemical Communications*, 46, (2010)  
652 412.  
653 [18] M. Tamura, K. Shimizu, A. Satsuma, *Applied Catalysis A: General*, 433, (2012) 135.  
654 [19] E. Furimsky, *Applied Catalysis A: General*, 199, (2000) 147.  
655 [20] C. Zhao, D.M. Camaioni and J.A. Lercher, *Journal of Catalysis*, 288, (2012) 92.  
656 [21] C. Zhao, J. He, A.A. Lemonidou, X. Li and J.A. Lercher, *Journal of Catalysis*, 280, (2011) 8.  
657 [22] J.R. Gasson, D. Forchheim, T. Sutter, U. Hornung, A. Kruse and T. Barth, *Industrial &*  
658 *Engineering Chemistry Research*, 51, (2012) 10595.  
659 [23] D. Forchheim, J.R. Gasson, U. Hornung, A. Kruse and T. Barth, *Industrial & Engineering*  
660 *Chemistry Research*, 51, (2012) 15053.  
661 [24] J. He, C. Zhao, D. Mei and J.A. Lercher, *Journal of Catalysis*, 309, (2014) 280.  
662 [25] S.R. Kirumakki, N. Nagaraju and S. Narayanan, *Applied Catalysis A: General*, 273, (2004) 1.  
663 [26] R. van Grieken, J.A. Melero and G. Morales, *Journal of Molecular Catalysis A: Chemical*, 256,  
664 (2006) 29.

665

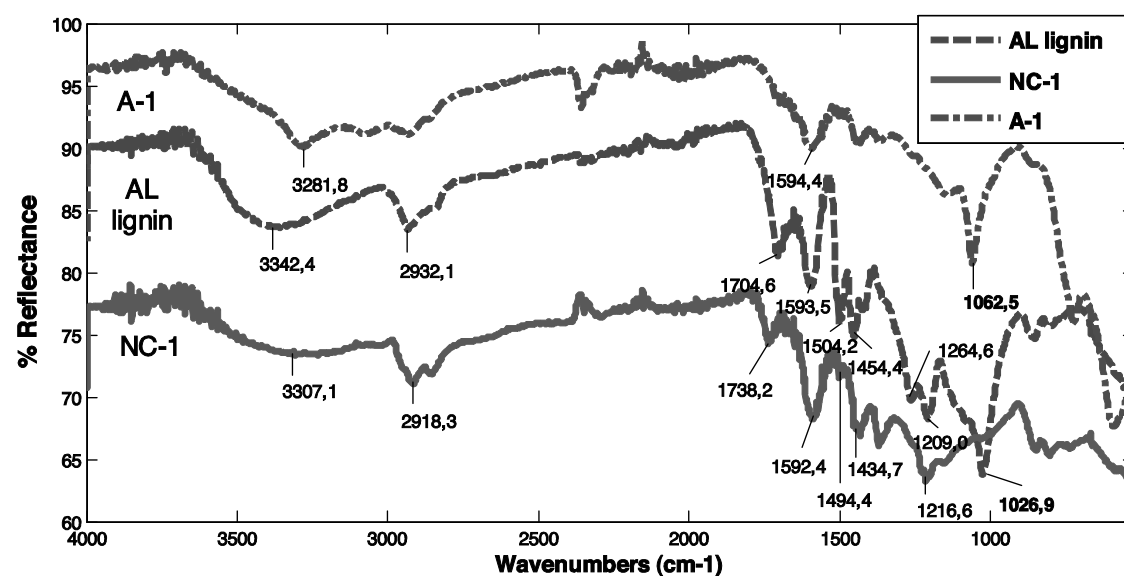
666



667

668 Fig. 1

669



670

671

672

673 Fig.2

674

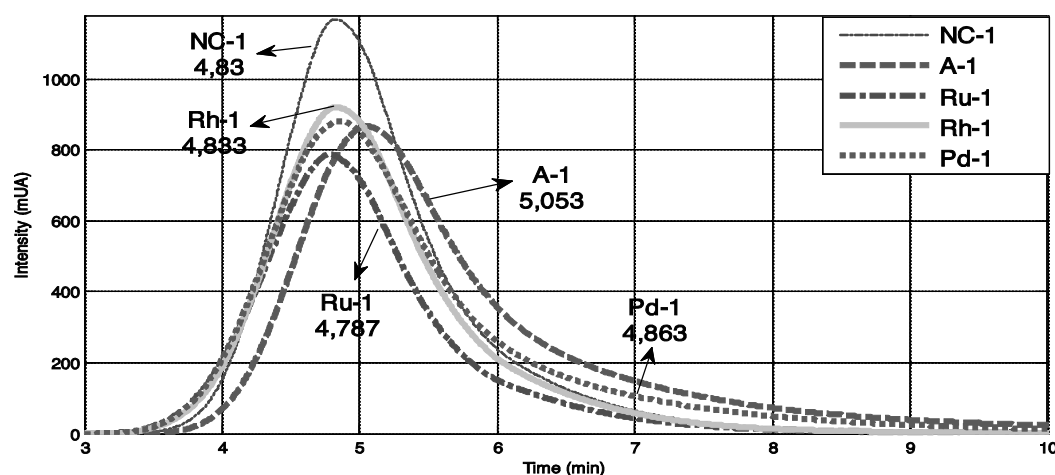
675

676

677

678

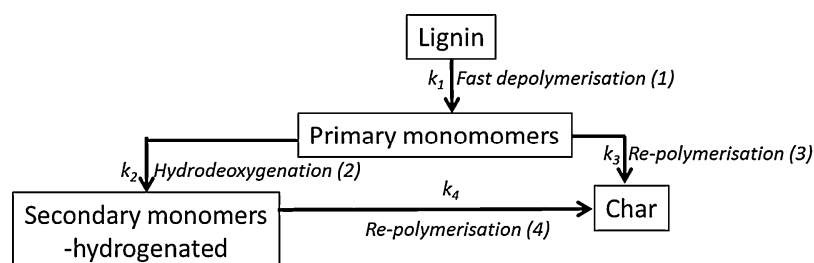




679

680 Fig. 3

681



682

683 Fig. 4

684

685 Table 1: Total acidity, acidityretention and active acidity of  $\gamma$ -alumina, Rh/ $\text{Al}_2\text{O}_3$ , Ru/ $\text{Al}_2\text{O}_3$  and  
686 Pd/ $\text{Al}_2\text{O}_3$ .

	Total acidity <sup>a</sup> (mmol $\text{NH}_3$ /g cat.)	Acidityretention <sup>b</sup> (%)	Active acidity (mmol $\text{NH}_3$ /g cat.)
<b><math>\gamma</math>-alumina</b>	1.51	100 (100°C) 92 (200°C) 92 (300°C)	1.51 (100°C) 1.39 (200°C) 1.39 (300°C)
<b>Rh/<math>\text{Al}_2\text{O}_3</math></b>	1.34	100 (100 °C) 71 (200°C) 49 (300°C)	1.34 (100°C) 0.95 (200°C) 0.66 (300°C)
<b>Ru/<math>\text{Al}_2\text{O}_3</math></b>	0.78	100 (100°C) 77 (200°C) 51 (300°C)	0.78 (100°C) 0.60 (200°C) 0.40 (300°C)
<b>Pd/<math>\text{Al}_2\text{O}_3</math></b>	0.76	100 (100°C) 99 (200°C) 98 (300 °C)	0.76 (100°C) 0.75 (200°C) 0.74 (300°C)

687 a) Data obtained from  $\text{NH}_3$ -TPD b) Data obtained from DRIFT

688

689 Table 2: Elemental composition of the altered and non-altered T316 stainless steel reactor surface

	Altered surface (%)	Non-altered surface (%)
<b>C</b>	32-45	0-4.8
<b>O</b>	28.5-32.5	0
<b>Si</b>	1.5-2.3	1
<b>Fe</b>	11-13	64-65
<b>Cr</b>	9.3-11.5	17
<b>Ni</b>	1.19-2.5	9-12
<b>Mo</b>	4.1-5.8	2.14-2.5
<b>Mn</b>	-	2-2.6

690

691 Table 3: Mass balance of the selected experiments at 340°C

Name of experiment	Oil Yield (% on lignin)	Solid Yield (% on lignin)	Gas phase (% total input)	Water Recovery (% initial input)	Lignin Mass Balance (%)	Total Mass Balance (%)
<b>NC-Q<sup>a</sup></b>	49.5	35.0	29.5	103.7	84.5	97.3
<b>NC-1<sup>a</sup></b>	58.2	22.4	30.5	103.6	80.6	97.9
<b>Ru-Q<sup>a</sup></b>	91.2	3.5	29.9	88.2	94.7	93.3
<b>Ru-1<sup>a</sup></b>	90.0	5.1	29.1	102.6	95.0	99.3
<b>A-1<sup>a</sup></b>	63.1	22.0	30.0	94.8	85.1	94.8
<b>Rh-1<sup>a</sup></b>	81.0	4.8	30.0	106.3	85.7	99.9
<b>Pd-1<sup>a</sup></b>	81.7	2.8	30.8	101.1	84.4	98.1

692 **NC:** non-catalyzed experiment. **A:**  $\gamma$ -alumina (0.2 g). **Rh:** rhodium on alumina (0.2 g). **Ru:** ruthenium on alumina (0.2 g). **Pd:** palladium on  
693 alumina (0.2 g). **Q:** A quartz insert was used to suppress the effect of the reactor wall **a)** **Reaction conditions:** 340°C and 6 h. 2 g of acid  
694 hydrolysis lignin, 5.0 g of water and 3.075 g of formic acid.

695 Table 4: Average oil and solid yields for the selected replicates

Name of experiment	Oil Yield (% on lignin)	Average Oil Yield and Standard deviation (%)	Solid Yield (% on lignin)	Average Solid Yield and Standard deviation (%)
<b>NC-1<sup>a</sup></b>	58.2	61.6±3.0	22.4	20.6±3.4
<b>NC-2<sup>a</sup></b>	62.3		23.0	
<b>NC-3<sup>a</sup></b>	64.2		16.5	
<b>A-1<sup>a</sup></b>	63.1	62.8±3.9	22.0	21.6±4.3
<b>A-2<sup>a</sup></b>	58.7		25.7	
<b>A-3<sup>a</sup></b>	66.5		17.1	
<b>Rh-1<sup>a</sup></b>	81.0	80.5±3.7	4.8	4.6±0.5
<b>Rh-2<sup>a</sup></b>	83.9		4.0	

<b>Rh-3<sup>a</sup></b>	76.6		5.0	
<b>Ru-1<sup>a</sup></b>	90.0	91.5±6.3	5.1	4.2± 1.0
<b>Ru-2<sup>a</sup></b>	98.4		4.4	
<b>Ru-3<sup>a</sup></b>	86.2		3.2	
<b>Pd-1<sup>a</sup></b>	81.7	82.9±2.2	2.8	2.7±0.3
<b>Pd-2<sup>a</sup></b>	85.4		2.4	
<b>Pd-3<sup>a</sup></b>	81.6		2.9	

696 **NC:** non-catalyzed experiment. **A:**  $\gamma$ -alumina (0.2 g). **Rh:** rhodium on alumina (0.2 g). **Ru:** ruthenium on alumina (0.2 g). **Pd:** palladium on  
697 alumina (0.2 g). **a) Reaction conditions:** 340°C and 6 h. 2 g of acid hydrolysis lignin, 5.0 g of water and 3.075 g of formic acid.

698

699 **Table 5:** Quantification of the main oil components by GC-FID and molecular weight distributions by  
700 GPC-SEC

GC-FID	<b>NC-1<sup>a</sup></b>	<b>A-1<sup>a</sup></b>	<b>Ru-1<sup>a</sup></b>	<b>Rh-1<sup>a</sup></b>	<b>Pd-1<sup>a</sup></b>	<b>NC-4<sup>b</sup></b>	<b>Ru-4<sup>b</sup></b>	<b>A-4<sup>b</sup></b>
<b>Phenol (wt % oil)</b>	1.68	1.44	1.99	1.41	2.47	2.70	1.52	1.56
<b>Cresol (wt % oil)</b>	3.62	3.16	4.27	2.94	5.22	5.90	3.17	3.41
<b>Guaiacol (wt % oil)</b>	2.53	2.18	3.21	2.03	3.44	4.22	2.28	2.42
<b>Methylguaiacol (wt % oil)</b>	2.38	2.29	2.80	1.91	3.38	3.92	2.13	2.58
<b>Catechol (wt % oil)</b>	2.00	3.15	1.91	1.35	2.05	3.68	1.70	3.35
<b>Ethylcatechol (wt % oil)</b>	1.36	3.24	1.44	0.99	1.69	2.33	1.36	3.76
<b>Syringol (wt % oil)</b>	0.19	0.20	0.22	0.12	0.23	0.47	0.19	0.26
<b>o-Vanillin (wt % oil)</b>	1.81	1.32	1.9	1.33	0	3.00	1.45	0
GPC-SEC	<b>NC-1<sup>a</sup></b>	<b>A-1<sup>a</sup></b>	<b>Ru-1<sup>a</sup></b>	<b>Rh-1<sup>a</sup></b>	<b>Pd-1<sup>a</sup></b>	<b>NC-4<sup>b</sup></b>	<b>Ru-4<sup>b</sup></b>	<b>A-4<sup>b</sup></b>
Average molecular weight (Da)	346	215	397	344	323	294	497	211

701 **NC:** non-catalyzed experiment. **A:**  $\gamma$ -alumina (0.2 g). **Rh:** rhodium on alumina (0.2 g). **Ru:** ruthenium on alumina (0.2 g). **Pd:** palladium on  
702 alumina (0.2 g). **a) Reaction conditions:** 340°C and 6 h. 2 g of acid hydrolysis lignin, 5.0 g of water and 3.075 g of formic acid. **b) Reaction**  
703 **conditions:** 380°C and 2 h. 2 g of acid hydrolysis lignin, 5.0 g of water and 3.075 g of formic acid.

704 **Table 6:** Results of the elemental analysis of the lignin, oils and solids

	<b>C (%wt)</b>	<b>H (%wt)</b>	<b>O (%wt)</b>	<b>N(%wt)</b>	<b>(O/C)</b>	<b>(H/C)</b>
<b>AL lignin</b>	61.27	5.74	32.82	0.16	0.40	1.12
<b>NC-1 Oil<sup>a,b</sup></b>	73.78	7.37	18.09	0.76	0.18	1.19
<b>A-1 Oil<sup>a,b</sup></b>	71.47	7.21	20.07	0.32	0.21	1.21
<b>Ru-10il<sup>a,b</sup></b>	74.29	7.31	17.86	0.54	0.18	1.17
<b>Rh-10il<sup>a,b</sup></b>	76.97	7.83	14.13	1.07	0.14	1.21
<b>Pd-10il<sup>a,b</sup></b>	76.97	7.83	14.13	1.07	0.14	1.21
<b>NC-1 Solid<sup>a,c</sup></b>	73.63	4.98	21.18	0.21	0.22	0.81

<b>A-1Solid<sup>a,c</sup></b>	42.60	3.46	53.82	0.12	0.95	0.97
-------------------------------	-------	------	-------	------	------	------

705 **NC:** non-catalyzed experiment. **A:**  $\gamma$ -alumina (0.2 g). **Rh:** rhodium on alumina (0.2 g). **Ru:** ruthenium on alumina (0.2 g). **Pd:** palladium on  
 706 alumina (0.2 g). **AL:** acid hydrolysis lignin **a) Reaction conditions:** 340°C and 6 h. 2 g of acid hydrolysis lignin, 5.0 g of water and 3.075 g of  
 707 formic acid. **b)** Elemental analysis of the oil. **c)** Elemental analysis of the recovered solids

708

709 **Table 7:** Composition of the gas phase for the selected experiments

	CO <sub>2</sub> (% mol)	CO (% mol)	H <sub>2</sub> (% mol)	CH <sub>4</sub> (% mol)	C <sub>2</sub> H <sub>6</sub> (% mol)	C <sub>3</sub> H <sub>8</sub> (% mol)	C <sub>4</sub> H <sub>10</sub> (% mol)
<b>NC-1<sup>a</sup></b>	59.50	7.95	31.33	1.01	0.12	0.04	0.05
<b>Ru-1<sup>a</sup></b>	60.69	2.97	34.74	1.35	0.13	0.06	0.06
<b>Pd-1<sup>a</sup></b>	62.80	3.34	31.39	2.11	0.15	0.08	0.13
<b>Rh-1<sup>a</sup></b>	63.99	3.67	29.88	2.10	0.16	0.09	0.12

710 **NC:** non-catalyzed experiment. **A:**  $\gamma$ -alumina (0.2 g). **Rh:** rhodium on alumina (0.2 g). **Ru:** ruthenium on alumina (0.2 g). **Pd:** palladium on  
 711 alumina (0.2 g). **a) Reaction conditions:** 340°C and 6 h. 2 g of acid hydrolysis lignin, 5.0 g of water and 3.075 g of formic acid.

712

713 **Table 8:** Mass balance and aqueous pH of experiment with different lignins at 380°C

Name of experiment	Type of lignin	pH (water phase)	Oil Yield (% on lignin)	Solid Yield (% on lignin)	Total Mass Balance (%)	Lignin Mass Balance (%)
<b>NC-4<sup>a</sup></b>	AL	4-5	54.0	26.3	99.1	80.2
<b>Rh-4<sup>a</sup></b>	AL	3-4	74.0	5.2	95.8	79.2
<b>Ru-4<sup>a</sup></b>	AL	4	83.9	8.2	102.3	92.1
<b>A-4<sup>a</sup></b>	AL	3-4	57.4	24.5	97.0	81.9
<b>NC-KL<sup>a</sup></b>	KL	8-9	47.9	10.4	90.2	58.3
<b>Rh-KL<sup>a</sup></b>	KL	8-9	52.3	10.0	92.8	52.3
<b>Ru-KL<sup>a</sup></b>	KL	8-9	44.7	6.9	89.0	51.6
<b>A-KL<sup>a</sup></b>	KL	8-9	47.0	11.7	92.8	58.7
<b>NC-EL<sup>a</sup></b>	EL	5	28.3	25.5	91.3	53.8
<b>Rh-EL<sup>a</sup></b>	EL	5	45.3	2.9	90.1	48.2
<b>Ru-EL<sup>a</sup></b>	EL	5	47.7	15.3	91.9	63.0
<b>A-EL<sup>a</sup></b>	EL	5	42.0	27.1	91.3	69.1

714 **NC:** non-catalyzed experiment. **A:**  $\gamma$ -alumina (0.2 g). **Rh:** rhodium on alumina (0.2 g). **Ru:** ruthenium on alumina (0.2 g). **Pd:** palladium on  
 715 alumina (0.2 g). **AL:** acid hydrolysis lignin. **KL:** kraft lignin. **EL:** enzymatic hydrolysis lignin **a) Reaction conditions:** 380°C and 2 h. 2 g of acid  
 716 hydrolysis lignin, 5.0 g of water and 3.075 g of formic acid.

717

718 **Table 9:** Gas, oil and solid yield for the high pressure and low pressure (LP) and **reduced catalyst**  
 719 **loading (LC)** experiments

Name of experiment	Oil Yield (% on lignin)	Solid Yield (% on lignin)	Gas phase (% total)	Lignin Mass Balance (%)
<b>NC-1<sup>a</sup></b>	58.2	22.4	30.5	80.6
<b>NC-LP<sup>b</sup></b>	29.9	44.9	33.4	74.7
<b>Ru-1<sup>a</sup></b>	90.0	5.1	29.1	95.0
<b>Ru-LP<sup>b</sup></b>	73.7	6.6	32.4	80.3
<b>Ru-LC<sup>a,c</sup></b>	85.2	4.5	30.0	89.7

720 **NC:** non-catalyzed experiment. **Ru:** ruthenium on alumina (0.2 g). **LP:** low pressure. **LC:** low catalyst content. **a)** **Reaction conditions:** 340°C  
 721 and 6 h. 2 g of acid hydrolysis lignin, 5.0 g of water and 3.075 g of formic acid. **b)** **Reaction conditions:** 340°C and 6 h. 1 g of acid hydrolysis  
 722 lignin, 2.5 g of water and 1.5375 g of formic acid and 0,1 g of catalyst. **c)** 0.1 g of catalyst

723

© 2015. This manuscript version is made available under the CC-BY-NC-ND 4.0 license <https://creativecommons.org/licenses/by-nc-nd/4.0/>(opens in new tab/window)